[1]Anbarasu P
[2]Loganathan N
[3]Narendran A
[4]Varatharaj M

Characterization and Modeling of Floating Photovoltaic Systems using MATLAB to support photovoltaic Sustainable Development

Journal of Electrical Systems

Abstract: - As a transformative advancement in energy production, floating photovoltaic (FPV) systems designed for water irrigation reservoirs have garnered significant attention due to their numerous advantages. The global clean energy community has shifted its focus towards these systems, recognizing their ability to conserve land, mitigate evaporation, and enhance power generation efficiency. Over the last decade, the FPV market has experienced remarkable growth, with its installed capacity doubling annually on a global scale. Specialists predict that this upward trend will persist, driven by the increasing significance of FPV systems as an alternative energy source. This research employs MATLAB tools to extract and model parameters missing from manufacturer datasheets, facilitating the integration of photovoltaic (PV) panels into FPV setups. Furthermore, the study investigates the impact of factors such as temperature variations and solar irradiance on PV panel performance. Consequently, experimental results underscore the enhanced efficiency of FPV systems deployed in water irrigation reservoirs.

Keywords: FPV, renewable energy, modeling, Single diode model, modeling algorithm, MATLAB/SIMULINK.

I. INTRODUCTION

Globally, there is a pressing need to augment energy consumption while concurrently diminishing dependence on fossil fuels, mitigating greenhouse gas emissions, and alleviating the impacts of global warming. This underscores the essentiality of proliferating alternative energy sources [1]. Among these alternatives, solar photovoltaic systems have emerged as a commendable option for meeting energy demands [2]. In the present era, solar energy emerges as a remarkably versatile resource, adept at meeting diverse requirements and serving as a reliable backup power option when contrasted with conventional energy sources [3]. PV energy systems are widely recognized for their ability to harness light energy and convert it into electricity [4]. In this field, FPV systems stand out as a notably advantageous utilization of PV technology, adept at reducing water evaporation while demonstrating impressive production capabilities. The swift advancement of this technology further emphasizes its potential [5].

Between 2009 and 2014, research was undertaken on FPV systems, encompassing various installations of FPV systems in South Korea [6]. In 2018, an examination focused on multiple FPV power configurations deployed on water surfaces, including pontoon systems. To enhance the production efficiency of these systems, several FPV projects have been suggested. The incorporation of functionalities such as cooling, tracking, and concentration has been meticulously analyzed, revealing their significant impact on system performance. Solar energy, available abundantly worldwide, underscores the potential of these advancements [7-8].

Therefore, the main aim of this research is to obtain missing parameters from the datasheet of manufacturer for a single diode model, and subsequently, to create a PV panel using MATLAB as a fundamental tool. Subsequently, this model is integrated into FPV systems, allowing for an examination of temperature and solar radiation impacts.

II. FLOATING PHOTOVOLTAIC COVER SYSTEM ARCHITECTURE

Floating Photovoltaic Cover System (FPVCS) presents a comprehensive solution aimed at enhancing the energy efficiency of agricultural canals. Comprising floating modules equipped with solar panels, this system addresses issues such as water loss through evaporation and algae proliferation by shading the water's surface, while simultaneously optimizing solar energy utilization. Key design elements crucial to its performance include the utilization of durable materials to ensure long-term sustainability and modularity, facilitating scalability and ease of maintenance. The structure of the FPVCS is illustrated in Fig.1.

[1] *Assistant Professor, Department of EEE, Sri Eshwar College of Engineering, Coimbatore, Tamil Nadu, India
[2] Assistant Professor, Department of EEE, Sri Krishna College of Engineering and Technology, Coimbatore, Tamil Nadu, India
[3] Assistant Professor, Department of EEE, SRM Madurai College for Engineering and Technology, Madurai, Tamil Nadu, India
[4] Associate Professor, Department of EEE, VSB College of Engineering Technical Campus, Coimbatore, Tamil Nadu, India

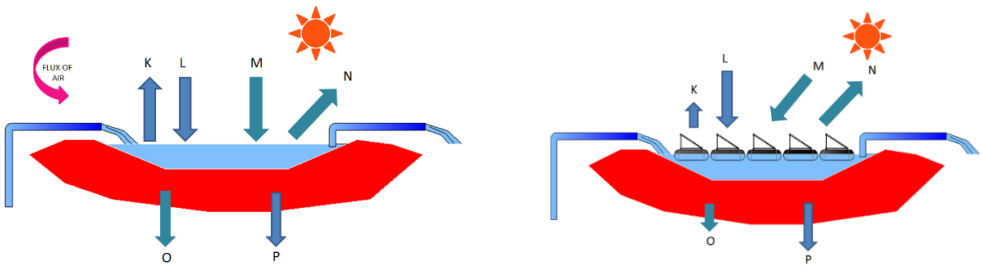

(a) Reservoir without Cover (b) Reservoir with PV Cover System

K – Evaporation, L – Rainfall, M – Radiation, N – Reflection, O – Heat Exchange, P – Seepage

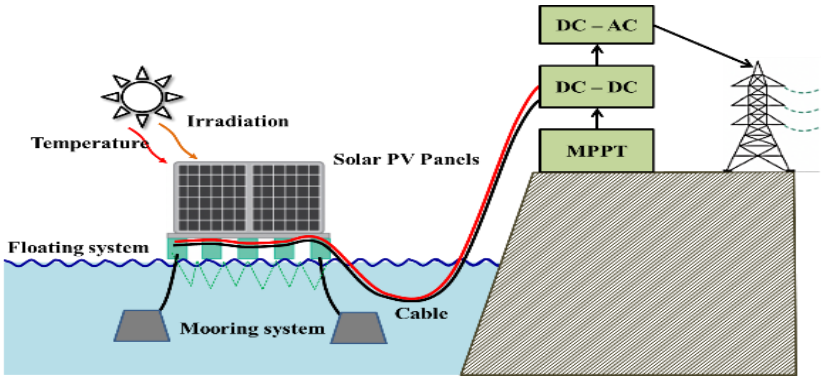

(c) Structure of proposed FPVCS

Fig. 1 Water and Energy Balance

The elements comprising an FPV system encompass cables, connections, the PV system, tie-up mechanisms, and a moving apparatus. A floater and supporting structure amalgamate to construct the floating system, with the PV system affixed atop it. Mooring serves to stabilize FPVCS components, preventing them from rotating or drifting. The PV system plays a pivotal role in converting light energy into electrical energy. Ongoing research endeavors aim to develop PV modules capable of adapting to the unique environmental conditions present in reservoirs or aquatic environments.

III. Modeling of Solar Photovoltaic Array

A PV array usually consists of multiple solar cells interconnected in parallel and series configurations. Common components found in the conventional solar cell model include reverse diodes and parallel-connected current sources.

A. Photovoltaic Cell Operation

Exposing light to the p–n junction of a semiconductor diode leads to the formation of a PV cell [9-10]. Fig. 2 offers a broad depiction of a PV cell's structure. When a photon with sufficient energy interacts with the semiconductor, it can cause the covalent electrons to separate, thereby generating charges.

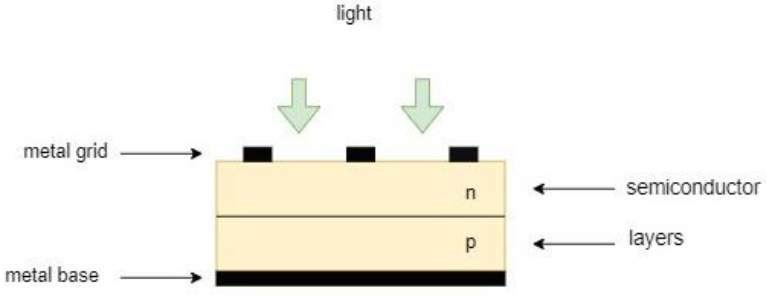

Fig. 2 PV cell structure

B. Modeling of Photovoltaic Parameters

1) Standard PV Cell

Fig. 3 depicts the standard PV cell's equivalent circuit, and the basic formula from the semiconductor principle that expresses the standard PV cell's current-voltage characteristic [11-12] mathematically is

$$I = I_{ph,c} - I_d \quad (1)$$

$$\text{Where,} \quad I_d = I_{o,c}\left[\exp\left(\frac{qV}{akT}\right) - 1\right] \quad (2)$$

From (1) & (2), we get

$$I = I_{ph,c} - I_{o,c}\left[\exp\left(\frac{qV}{akT}\right) - 1\right] \quad (3)$$

where p–n junction temperature is expressed as T (in K), incident light's produced current is denoted as $I_{ph,c}$, k is Boltzmann constant ($1.3806503 \times 10^{-23}$ J/K), Shockley diode equation is indicated as I_d, is the diode's reverse saturation or leakage current as $I_{0,c}$, charge of electron as q ($1.60217646 \times 10^{-19}$ C), and diode ideality constant as a. The I-V curve is originated from (1) is indicated in Fig.4

In practical setups, arrays consist of multiple interconnected PV cells, necessitating the incorporation of supplementary parameters into the fundamental ideal equation to accurately observe the characteristics at the array terminals. Therefore, it may be stated as

$$I = I_{ph} - I_o\left[\exp\left(\frac{V+R_sI}{V_ta}\right) - 1\right] - \frac{V+R_sI}{R_{sh}} \quad (4)$$

In this context, R_s represents the equivalent series resistance, while R_{sh} represents the equivalent parallel resistance of the array. The equation described above forms the basis for the I-V curve depicted in Fig. 5, with the maximum power point (MPP) highlighted. The current generated by the PV cell in response to light intensity varies linearly with solar irradiance and is also impacted by temperature, as described by the following equation,

$$I_{ph} = (I_{ph,nc} + K_I\,\Delta T)\frac{G}{G_n} \quad (5)$$

Here G (W/m^2) is the device surface's irradiation, $\Delta T = T - T_{nc}$ (T_{nc} [K] be the nominal temperature and T [K] be the actual temperature), $I_{ph,nc}$ is the current generated by light at the standard circumstances (generally 1000 W/m^2 and 25^0C) and G_{nc} is the standard irradiation. The nominal saturation current, $I_{0,nc}$ is expressed by as in [13-15].

$$I_{o,nc} = \frac{I_{sc,nc}}{\exp\left(\frac{V_{oc,nc}}{a\,V_{t,nc}}\right) - 1} \quad (6)$$

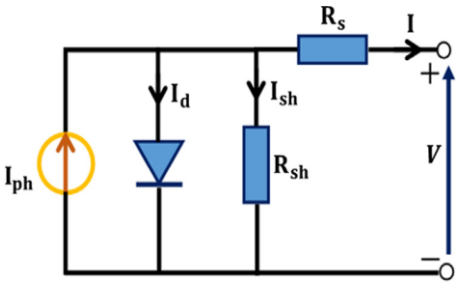

Fig. 3 PV device's circuit diagram

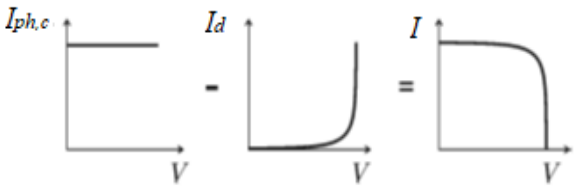

Fig. 4 Characteristic I-V curve of PV cell

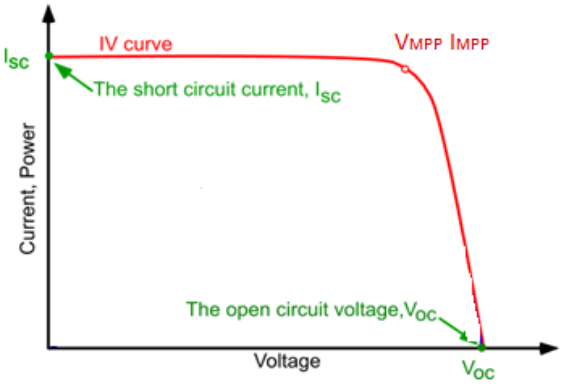

Fig. 5 Practical PV device's characteristic curve

2) Modifying the Model

Enhancing the PV model that was previously discussed in the section by

$$I_o = \frac{I_{sc,nc} + K_I \Delta T}{\exp\left(\frac{V_{oc,nc} + K_V \Delta T}{a V_{t,nc}}\right) - 1} \quad (7)$$

Equation (7) is formulated by augmenting (6) with the K_I and K_V. The purpose of this adjustment is to align the V_{oc} of the model with experimental data over a wide range of temperatures.

3) Adapting the Model

To achieve the desired alignment between the model's experimental data, P-V and I-V curves, the appropriate values for R_s and R_{sh} can be determined by equating $P_{max,mp}$ to $P_{max,ep}$. The resultant expression for R_s can then be solved as below

$$P_{max,mp} = V_{mpp}\left\{I_{ph} - I_o\left[\exp\left(\frac{q}{k\,T}\frac{V_{mpp} + R_s I_{mpp}}{a\,N_s}\right) - 1\right] - \frac{V_{mpp} + R_s I_{mpp}}{a\,N_s}\right\} = P_{max,ep} \quad (8)$$

$$R_{sh} = V_{mpp}\,(V_{mpp} + I_{mpp}\,Rs) / \left\{V_{mpp} I_{pv} - V_{mpp}\,I_o \exp\left(\frac{q}{k\,T}\frac{V_{mpp} + R_s I_{mpp}}{a\,N_s}\right) + V_{mpp} I_o - P_{max,ep}\right\} \quad (9)$$

From the above expression, for every R_s value, equivalent R_{sh} is available such that the mathematical current-voltage curve crosses the experimental (V_{mpp}, I_{mpp}) point. The determination of the P-V curve necessitates exploring various ranges of R_s and R_{sh} to ensure alignment with the actual data.

The model refined through previous steps undergoes further enhancement via a modeling algorithm, leveraging the iterative solution of resistances R_s and R_{sh}, illustrated in Fig.6. This algorithm adjusts existing models by integrating empirical data and insights gathered from experiments. They employ methodologies derived from computational optimization, machine learning, and data-driven analyses to fine-tune model parameters and enhance predictive capabilities.

The introduction of these modeling algorithms signifies a significant progression in PV system engineering. By amalgamating empirical data with computational methodologies, these algorithms enable more precise forecasts of PV module performance across a diverse array of operating conditions.

In each iteration, R_s and R_{sh} are adjusted iteratively near the optimal model solution, thus introducing (10) into the model.

$$I_{ph,nc} = \frac{R_s + R_{sh}}{R_{sh}} . I_{sc,nc} \quad (10)$$

Starting with R_s set to zero, the initial value of R_{sh} is determined by

$$R_{sh,min} = \frac{V_{mp}}{I_{sc,nc} - I_{mp}} - \frac{V_{oc,nc} - V_{mp}}{I_{mp}} \quad (11)$$

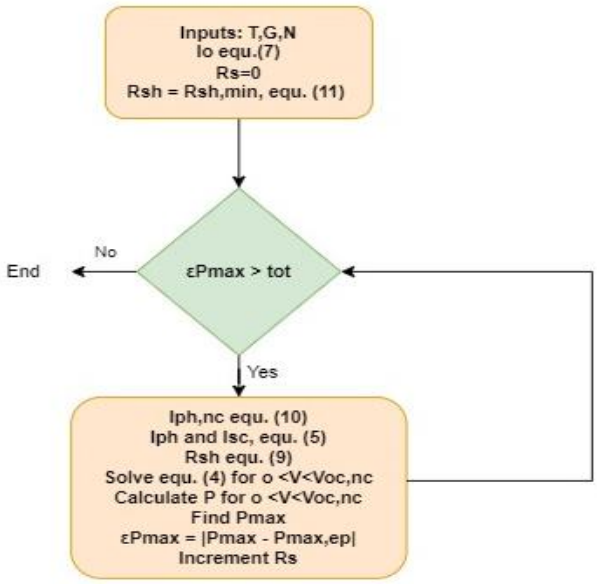

Fig.6 Modeling Algorithm to modify I-V model

The PV(SSS-330) Solar arrays I-V and P-V features across different irradiation levels are illustrated in Fig.7. The value of PV panel from customer data sheet is shown in Table 1. It clearly depicts the value of R_s and R_{sh} are missing.

The values obtained from the modelling algorithm are used to simulate the proposed method in SIMULINK as shown in Fig.8. It presents the simulation model exhibits suitability for a comprehensive collection of solar array configurations.

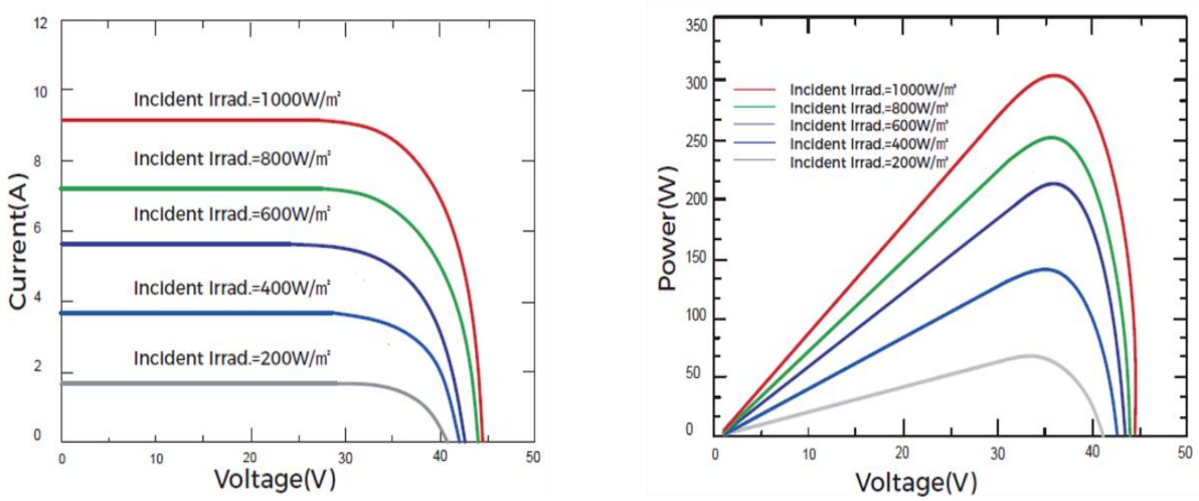

Fig.7 Characteristics of a PV(SSS-330) solar module

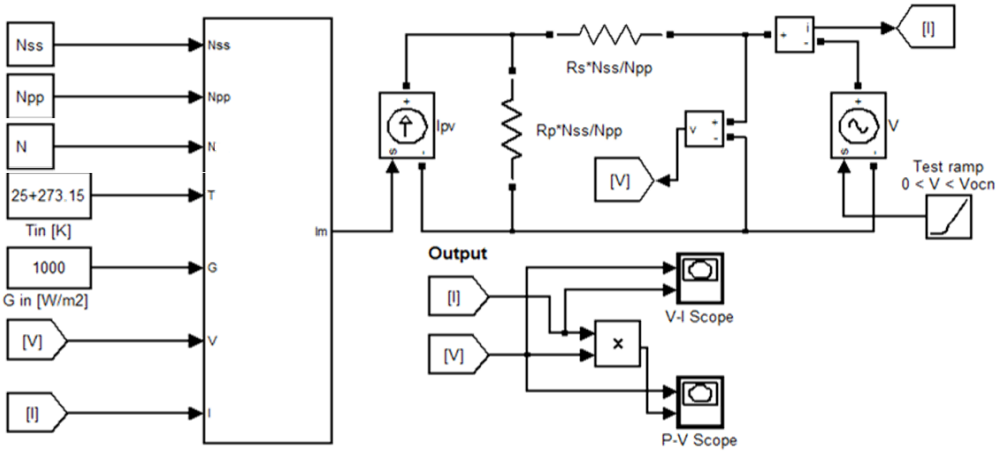

Fig. 8 Simulink Model of the Proposed FPV System

Table. 1 Constraints of the PV(SSS-330) Solar Array at 25˚C A.M 1.5 1000 W/m^2.

Description	Values
$V_{oc,n}$	46.08 V
$I_{sc,n}$	8.92 A
V_{mp}	38.95 V
I_{mp}	8.48 A
$P_{max,e}$	330 W
K_i	0.04 % / ˚C
K_v	-0.31 % / ˚C

The values that are missing in manufactures data are identified using modelling algorithm, except diode ideal factor ‘a’. The values identified using this algorithm is shown in Table. 2.

Table. 2 Constraints of the Modified Model of PV(SSS-330) Array at Normal Working Conditions

Description	Values
$V_{oc,n}$	46.08 V
$I_{sc,n}$	8.92 A
V_{mp}	38.9 V
I_{mp}	8.48 A
$I_{o,n}$	2.90204x10-10 A
$P_{max,e}$	330 W
a	1
I_{pv}	8.950 A
R_{sh}	65.570456 Ω
R_s	0.438800 Ω

IV. SIMULATION RESULTS

The proposed system with 6 solar modules, capable of generating 2 kW of electricity is shown in Fig. 13. The panels are organized in a configuration consisting of one parallel combinations, with each combination having six panels connected in series (N_{ss} = 6) and four combinations connected in parallel (N_{pp} = 1). This arrangement is chosen to achieve the desired voltage and current specifications. The input parameters outlined for the solar panel, as depicted in Table. 1, serve as the inputs for the Simulink model. This facilitates the generation of a design and enables an analysis of the anticipated output characteristics of the proposed system.

The Power-Voltage and Current-Voltage curves from the simulation results are displayed in Fig. 9 and Fig. 10 for a variety of temperatures at 1000 W/m^2. The variations seen at various irradiation intensities at a temperature of 25°C are illustrated in Fig.11 and Fig.12. The simulation findings presented in this study contribute to the implementation of FPV.

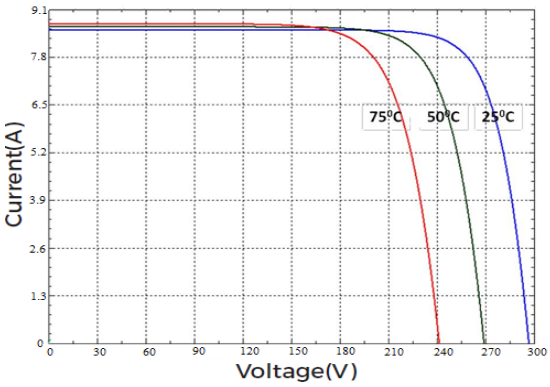

Fig. 9 Current-Voltage curve at 1000 W/m^2 for different temperature levels

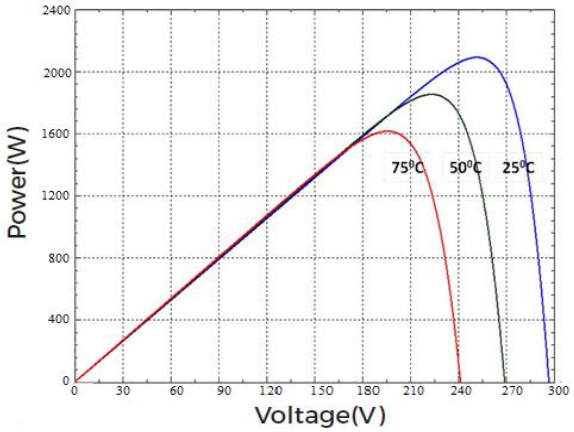

Fig.10 Power-Voltage curve at 1000 W/m^2 for different temperature levels

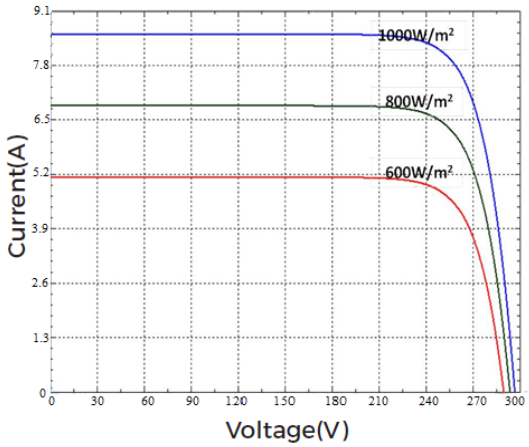

Fig. 11 Current-Voltage Curve at 25˚C for different irradiation Levels

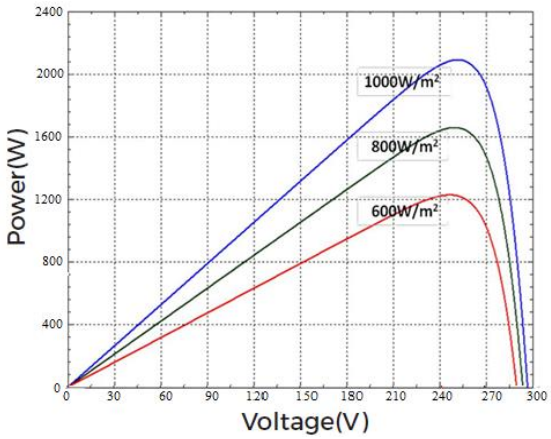

Fig. 12 Power-Voltage Curve at 25˚C for different irradiation Levels

Th solar array output of 2 kW system was measured along with the load setup with different irradiance, temperature and angle variation are shown in Table. 3. The 3D view of proposed model is in Fig. 13 with a total area of 144 m^2. Approximately 20% of the water surface was used as a full-scale prototype to verify system operation and make appropriate testing and engineering modifications. The overall performance of the prototype has been satisfactory with an annual energy efficiency of 1600 kWh. The FPV system has an area of 29 m^2 (20% of the reservoir water surface area) corresponding to a maximum installed capacity of 2 kW. The ideal tilt angle for a fixed solar PV system is 18° for obtaining maximal power generation. However, a small tilt angle will reduce the impact of wind lift and drift on the solar PV system. Since the whole system's structural performance is greatly influenced by wind speed. As a result, using a low tilt angle increases system performance. The system comprises of a floating module measuring 21 * 8 m, which serves as a support net. There are 6 modules, each module is connected to adjacent modules by a connector. The frame is made of stainless steel with corrosion resistance. Corrosion of stainless steel is not affected at all. The material has the ability to self-repair, so even if damaged, the surface will not corrode or change color. Metal anchors are used to secure the joints of each frame together. Above the water tank, the bases are fixed. The solar panel mounting structure is placed over the pontoon and fixed to the rail with a help of metallic pin-anchorage.

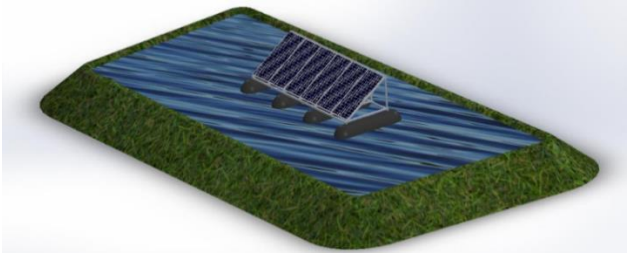

Figure 13. Installed structure of FPVCS

Table 3. Simulink Output of 2kW FPV System

Time	Temp (℃)	Irradiation (w/m^2)	Angle Variation (Degree)	Solar		Load		
				Power (kW)	Current (A)	Power (kW)	Current (A)	Voltage (V)
09.00 a.m	26.3	250	20	0.5	2.5	0.5	2.2	223
10.00 a.m	27.2	520	25	1.2	5.9	1.1	5.2	218
11.00 a.m	28.6	630	32	1.2	6.6	1.0	4.8	225
12.00 p.m	28.9	640	36	1.4	6.8	1.1	6.0	235
01.00 p.m	31.6	650	40	1.8	7.8	1.2	6.8	234
02.00 p.m	29.8	570	47	1.6	7.8	1.4	7.0	236
03.00 p.m	28.6	480	52	1.5	6.1	1.3	5.8	231
04.00 p.m	27.3	310	56	0.9	3.2	0.5	2.3	220

V. CONCLUSION

This paper has investigated the mathematical model for Floating Photovoltaic system. FPV array series and parallel connections are considered in solar irradiance and temperature models. A technique has been put forward to correspond with the experimentally notable points of the practical array's current-voltage curve to the mathematical I-V equation. The proposed method equals maximum powers of the model and the practical array to determine the unknown parameters from manufactures datasheet. Current sources, diodes, and resistance factors simulate solar cells. Testing and verification of the model is performed with MATLAB/Simulink.

REFERENCES

[1] Das, U. K, et al., "Forecasting of photovoltaic power generation and model optimization: A review," Renewable and Sustainable Energy Reviews, vol. 81, pp. 912-928, 2018.

[2] Gholami, H., Khalilnejad, A., Gharehpetian, G. B., "Electrothermal performance and environmental effects of optimal photovoltaic–thermal system," Energy conversion and management, vol. 95, pp. 326-333, 2015.

[3] Ram, J. P., Babu, T. S., Rajasekar, N., "A comprehensive review on solar PV maximum power point tracking techniques," Renewable and Sustainable Energy Reviews, vol. 67, pp. 826-847, 2017.

[4] Kumari, P. A., Geethanjali, P., "Parameter estimation for photovoltaic system under normal and partial shading conditions: A survey," Renewable and Sustainable Energy Reviews, vol. 84, pp. 11, 2018.

[5] Zhou, X., Yang, J., Wang, F., Xiao, B., "Economic analysis of power generation from floating solar chimney power plant," Renewable and Sustainable Energy Reviews, Vol. 13, No. 4, pp. 736-749, 2009.

[6] Trapani, K., Millar, D. L., "Proposing offshore photovoltaic (PV) technology to the energy mix of the Maltese islands," Energy Conversion and Management, Vol. 67, pp. 18-26, 2013.

[7] Shahinpour, A., Moghani, J. S., Gharehpetian, G. B., Abdi, B., "High gain high-voltage z-source converter for offshore wind energy systems. In the 5th annual international power electronics," Drive Systems and Technologies Conference (PEDSTC 2014), IEEE., pp. 488-493, 2014.

[8] Maghrebi, M. J., Nejad, R. M., "Performance evaluation of floating solar chimney power plant in Iran: Estimation of technology progression and cost investigation," IET Renewable Power Generation, vol. 11, no. 13, pp. 1659-1666, 2017.

[9] Mittal, D., Saxena, B. K., Rao, K. V. S., "Floating solar photovoltaic systems: An overview and their feasibility at Kota in Rajasthan," In 2017 International Conference on Circuit, Power and Computing Technologies (ICCPCT), IEEE., pp. 1-7, 2017.

[10] Astuti, Y. D. R. W., Hudaya, C., Putri, R. K., Sommeng, A. N., "Photovoltaic installation in Floating Storage and Offloading (FSO) vessel," In 2018 2nd International Conference on Green Energy and Applications (ICGEA), IEEE., pp. 119-123, 2018.

[11] El Hammoumi, A., Motahhir, S., Chalh, A., El Ghzizal, A., Derouich, A., "Low-cost virtual instrumentation of PV panel characteristics using Excel and Arduino in comparison with traditional instrumentation", Renew. Wind, Water, Sol. Vol. 5, no.1, pp. 3, 2018.

[12] R. S. Kumar, "Performance analysis of polycrystalline floating photovoltaic array: The concept and prototype development for irrigation purpose," in progress in photovoltaics, vol. 31, pp. 738–749, July 2023.

[13] S. B. S, P. N, K. M, R. K, S. D and R. S, "Monitoring System for Water Quality Using Solar Powered IoT," 2022 8th International Conference on Smart Structures and Systems (ICSSS), Chennai, India, pp. 1-4, 2022.

[14] P. Abijith, M. Balasuryaprakash, S. Harrish, S. Yokesh Kumar, K. Raj Thilak and N. Franklin, "A Methodological Approach for The Dual Axis Solar Tracking System," 2022 8th International Conference on Advanced Computing and Communication Systems (ICACCS), Coimbatore, India, pp. 1836-1839, 2022.

[15] E. I. Ortiz-Rivera and F. Z. Peng, "Analytical model for a photovoltaic module using the electrical characteristics provided by the manufacturer data sheet," in Proc. IEEE 36th Power Electron. Spec. Conf. (PESC), pp. 2087–2091, 2005.